Journal of Nuclear Materials 555 (2021) 153140

Contents lists available at ScienceDirect

Journal of Nuclear Materials

journal homepage: www.elsevier.com/locate/jnucmat

Improving radiation-tolerance of bcc multi-principal element alloys by tailoring compositional heterogeneities

Hongjiang Li, Long Zhao, yang Yang, Hongxiang Zong*, Xiangdong Ding*

State Key Laboratory for Mechanical Behavior of Materials, Xi'an Jiaotong University, Xi'an, Shanxi 710049, China

ARTICLE INFO

Article history:
Received 26 February 2021
Revised 8 May 2021
Accepted 4 June 2021
Available online 17 June 2021

Keywords:
Radiation damage
High entropy alloy
Refractory alloy
Atomistic simulation

ABSTRACT

Molecular dynamic simulations were performed to investigate the displacement cascade process in refractory bcc complex concentrated alloys, including equi-atomic binary, ternary, and quaternary systems made of the elements Mo, Nb, Ta and W. Our simulation results show that more principal elements do not necessarily mean better radiation resistance. Instead, bcc binary MoNb and NbW CCAs, which have low binding energy of interstitial clusters, can also yield good resistance to the generation of radiation-induced defect clusters. At same time, MoNb also have low self-interstitial formation energy range, so there are more Frenkel Pairs than other bcc binary like MoTa and MoW although number of interstitials in clusters of MoNb is least. More importantly, we find the binding energy of interstitial clusters is highly tunable by changing elements combination and tailoring compositional heterogeneities (such as short-range ordering). Such strategies may pave the way for new design concepts of radiation-tolerant alloys.

1. Introduction

Complex concentrated solid-solution alloys including high-entropy alloys (HEAs) have emerged as a relatively new category of materials due to their structural stability and excellent mechanical properties [1,2]. These alloys are, in principle, single-phase crystalline solid solutions comprising multiple elements, typically in equi-atomic or nearly equi-atomic ratios. Intense recent works have revealed that complex concentrated alloys (CCAs) have the ability to maintain good mechanical properties [3,4]. Hence, they are strong candidates to resolve many challenges imposed by extreme environments. In particular, increasing experimental studies show that most CCAs exhibit high radiation damage tolerance [5-8], making them potential candidates for the next-generation nuclear materials.

There is an idea that the high radiation damage tolerance of CCAs mainly originates from the altering of defects migration dynamics by their multiple components and special chemical structure. On the one hand, the compositional and configurational complexities endow CCAs with considerable local lattice distortion that further complicates the energy landscape for defect migration [9,10]; On the other hand, CCAs are thought to possess slow energy dissipation ability, i.e., concentrated solid-solution alloys exhibits a substantially long lifetime of thermal spikes in a cascade, which can enhance Frenkel pairs recombination [11,12]. Therefore, the materials show better radiation resistance with the increase of principle elements [13,14]. Although this idea is supported by previous studies, there is not enough mechanistic underpinnings to state as fact yet. What's more, these results are mainly inferred from the observation on Ni-based fcc HEAs [15-17], while it is unclear whether it is the same true for other complex concentrated alloy systems, such as bcc CCAs.

It is theorized that defect migration dynamics is correlated with the local atomic environment, which significantly influence the migration energy barriers and pathways of radiation defects. This has been demonstrated by a lot of studies [18-20] which tune the radiation damage tolerance of CCAs by varying alloy elemental concentrations and types. In the simplest description, the local chemical environments of HEAs can be considered as representing a random distribution of different atomic species over crystal lattice sites, i.e., the chemical concentration is quite homogenous over the alloy system. As of today, such a random solid-solution picture remains a common assumption in the high-entropy alloy community. However, an increasing body of evidence suggests that there be appreciable inhomogeneity statistically fluctuating from one place to another, in compositional arrangements, not to mention local chemical order (i.e., ordering in the first few neighbor atomic shells to enhance the number of energetically preferred bond types) [21,22]. In this sense, the compositional heterogeneity can be tuned over a wide range, thus have potential of serving as a freedom to tailor

* Correspondence author.
E-mail addresses: zonghust@mail.xjtu.edu.cn (H. Zong), dingxd@mail.xjtu.edu.cn (X. Ding).

https://doi.org/10.1016/j.jnucmat.2021.153140
0022-3115/

the radiation tolerance of the CCAs. The motivation of this work is to figure out how could compositional heterogeneity affect the radiation induced defect generation in refractory bcc CCAs, and what are the underlying parameters influencing their radiation tolerance?

Here we take the Mo-based CCAs, which a competitive candidate to replace Zr alloy fuel cladding in fusion reactor [23,24], as an example to study the primary radiation damage by utilizing molecular dynamics (MD) simulations. The radiation damage accommodation mechanisms of equi-atomic binary, ternary, and quaternary Mo alloys, which are concentrated alloyed with the elements of Nb, Ta or W, are systematically compared to uncover the key factors governing the radiation tolerance. Our simulation results show that besides local lattice distortion and slow energy dissipation, the alloying elements and compositional heterogeneity also play an important role in suppressing the formation of defect clusters, and can be used to tailor the radiation tolerance of bcc CCAs. It provides new aspects for us to understand the effect of concentrated solid-solution on radiation damage.

2. Methodology

To investigate the radiation damage behavior of bcc CCAs, we performed molecular dynamic (MD) simulations of singe crystal samples of different CCAs. These CCAs systems include equial-atomic MoNb, MoTa, MoW, MoNbTa and MoNbTaW, we also investigate the radiation damage behavior of pure Mo and Nb as reference. The initial bcc samples were constructed by randomly-filling sites with specific atoms at the equi-atomic compositions. The simulations employed embedded atom model (EAM) potential parameters of Zhou et al. [25] and Lin et al. [26]. Previous MD simulations of bcc high-entropy alloys using these potentials reproduced key aspects of the mechanical behaviors [27-29]. Besides, Ziegler-Biersack-Littmark (ZBL) repulsive potential [30] was used to modify the current EAM potential when the distance between two atoms is smaller than 2 Å. A switch function [31] is added to smooth the ZBL resulsive potential and the original EAM potential in the range of 1~2 Å. Two simulation boxes in dimension of $75a_0 \times 75a_0 \times 75a_0$ (843,750 atoms) and $100a_0 \times 100a_0 \times 100a_0$ (2,000,000 atoms) (a_0 is lattice constant) were used to simulate the primary radiation damage event under the Primary knock-on atoms (PKA) energies of 30 keV and 50 keV, respectively. Periodic boundary conditions were applied along all directions. Before the cascade simulation, samples were first relaxed in a NPT ensemble at 300 K to reach a equilibrium state (see in supplementary material). For each cascade simulation, a PKA was selected randomly at the center of the sample with a constant kinetic energy of 30 keV or 50 keV and random knock-on direction. It is followed by the microcanonical (NVE) ensemble in the core region while a Berendsen thermostat in the edge area within 0.5 nm width. Adaptive time step algorithm [32] was used to ensure the accuracy of the integration at initial cascade process. To reach the stable state, the MD runs until the global temperature return to 300 K without significant energy fluctuations (after 100 ps~400 ps, see in supplementary material). For each case, we repeated 20 times to check the reliability of our simulation results, and the corresponding numbers of defects were also averaged over 20 cascade simulations. Here, all the MD simulations were carried out using the LAMMPS package [33]. Open Visualization Tool (Ovito) [34] is applied to extract Frenkel pairs by the integrated Wigner-Seitz method [35]. Accordingly, the interstitial clusters are then identified based on the neighboring criterion (less than second nearest distance in the present work) [36]. Also, we use dislocation extraction algorithm(DXA) [37] to analysize involved dislocations.

To investigate the effect of local chemical concentration on radiation resistance, the Monte Carlo [38] simulation was carried out to obtain equilibrium configurations after annealing at room temperatures. Upon annealing, the local chemical short-range order can change with time. Here, the Warren-Cowley pairwise short-range-order parameter α_{ij}^{m} was calculated to quantify the degree of short-range order, where superscript m means m-th nearst neighbor shell of central atom, subscript i, j represent the types of central atom and neighbor atom, respectively [39].

Besides, the self-interstitial formation energy as well as the interstitial cluster binding energy are also calcuated in the present work. Here, the self-interstitial formation energy is defined as $E_i = E_2 - \frac{N+1}{N} * E_1$, where E_1 is the energy of a perfect CCA, E_2 is the energy after inserting a guest atom into a selected interstitial position, and N is total number of atoms. While the binding energy of interstitial clusters with different sizes is calculated by $E_b^{i_1,i_2,\ldots,i_n} = \sum_{j=1}^{n} E_f^{i_j} - E_f^{i_1,i_2,\ldots,i_n}$, where $E_f^{i_j}$ is the formation energy of system only contain an interstitial atom j, and $E_f^{i_1,i_2,\ldots,i_n}$ is the formation energy of a interstitial cluster with n different interstitial atoms [40].

3. Results

Previous studies on Ni-containing equi-atomic fcc alloys and CCAs have suggested that increasing the number of principal elements can enhance the compositional complexity, which can modify defect dynamics to promote annihilation of radiation damage that ultimately enhance radiation tolerance [11]. Besides, the generation, distribution and evolution of defects in the early stage of displacement cascades are important information for obtaining the mechanisms of irradiation resistance [41,42]. Therefore, we first investigate the radiation induced defect formation upon a displacement cascade for bcc CCAs with different numbers of principal elements. As shown in Fig. 1, the surviving defect data are compared among pure Mo, MoNb, MoNbTa and MoNbTaW CCAs. For both 30 keV and 50 keV displacement cascade cases, the number of surviving Frenkel pairs and interstitials in clusters are generally less than that in fcc CCA systems [11], indicating a better performance of bcc CCA systems [43,44]. More importantly, we find that it is not always true that more surviving Frenkel pairs means more interstitials aggregate to form clusters in bcc CCAs. For example, the number of Frenkel pairs in MoNb is more than that of pure Mo(Fig. 1(a) and (b)), but the number of interstitials in clusters is less in both cascades of 30 keV and 50 keV(Fig. 1(c) and (d)). However, further complicating the composition to MoNbTa and MoNbTaW decreases both Frenkel pairs and interstitials clusters.

More strikingly, the CCAs exhibit excellent resistance to the formation of interstitial clusters compared to elemental materials. At 30 keV, there are around 12 mean number of interstitial atoms in the size of 2–10 clusters in pure Mo. It is more than twice as many as that in other three CCAs. The difference in the size of 11–30 clusters is tinny for all the metallic materials. Note that the binary MoNb CCA has shown a good enough suppressed interstitial atoms accumulation, i.e., the total number of interstitials within the clusters of all sizes is reduced by over 50%. The same is true for 50 keV displacement cascade cases where the capability of resisting interstitial clusters formation in pure Mo is obviously worse than that of other three CCAs, as shown in Fig. 1(d). We note that the defect-cluster reduction among CCAs between 30 keV and 50 keV is a bit different (see Table 1), i.e., the effect of composition complication is stronger when undergone higher PKA energy cascade.

In Fig. 2, the typical morphology of surviving defects of pure Mo and the three CCAs for 50 keV radiation case are visualized. The red and purple atoms present the self-interstitial atoms and vacancies respectively. In each case, we can find large interstitial clusters, which act as a precursor of dislocations, demonstrated by

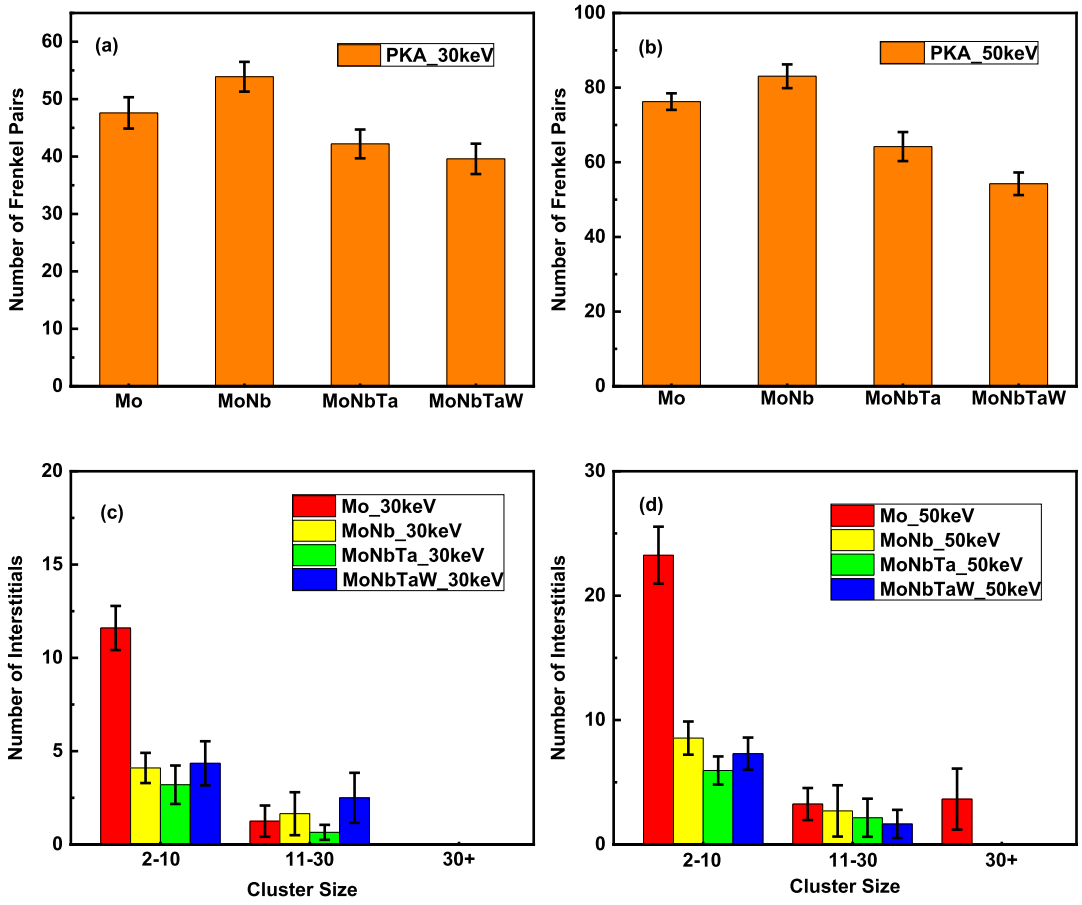

Fig. 1. Comparison of irradiation-induced damage in elemental Mo and MoNb, MoNbTa, MoNbTaW CCAs. (a-b) Number of surviving Frenkel pairs at cascade energy of 30 keV and 50 keV. (c-d) Number of interstitials in different sizes clusters at cascade energy of 30 keV and 50 keV.

Table 1
Averaged defect number after PKA for Mo, MoNb, MoNbTa and MoNbTaW.

E_{PKA}(eV)	Element composition	Frenkel pairs	Interstitials in clusters(size:2–10)	Interstitials in clusters(size:11–30)	Interstitials in clusters(size:30+)
30keV	Mo	47.6	11.6	1.3	0
	MoNb	53.9	4.1	1.7	0
	MoNbTa	42.2	3.2	0.7	0
	MoNbTaW	39.6	4.4	2.5	0
50keV	Mo	76.3	23.3	3.3	3.7
	MoNb	82.9	8.1	2.8	0
	MoNbTa	64.2	6.0	2.2	0
	MoNbTaW	54.3	7.3	1.7	0

1/2⟨111⟩ dislocation loops formed around these interstitial clusters. In this aspect, it is consistent with previous studies that the clustering of self-interstitial atoms predominate the formation of dislocations in bcc alloy systems [45]. Hereafter, we will mainly focus on the information of radiation-induced interstitial clusters.

We find the suppression of interstitial atoms accumulation in binary systems depends on the chemical composition (alloying elements) seriously. Fig. 3 compares the Frenkel pairs and interstitial clusters formation behaviors of three Mo-based binary CCAs i.e. MoNb, MoTa and MoW. The three binary CCAs have similar compositional complexity, but the number of Frenkel pairs in MoNb is obviously more than that in MoTa and MoW at 30 and 50 keV (see Fig. 3(a) and (b)). Nevertheless, in Fig. 3(c) and (d), we show the ability of suppressing interstitial clusters in MoNb CCA still outperforms other two CCAs, and this is demonstrated by showing less interstitials in clusters. In contrast, MoW CCA has the worst ability to resist interstitial clusters formation, while MoTa CCA in between. Summarizing the results shown in Fig. 3 , the relative interstitial clusters forming resistance of these three CCAs can be ranked in the order from the worst to the best as MoW< MoTa < MoNb. However, like the result in Fig. 1, the MoNb CCA resides the most Frenkel pairs. This is quite different from normal cases where the more interstitial atoms, the greater chance of forming interstitial clusters. It seems that alloying element Nb can dictate the interstitial atoms that are unwilling to agglomerate together. The specific element seems play a significant role here.

Therefore, we investigated the effect of Nb concentration on the primary radiation damage behavior. Fig. 4 compares the number of Frenkel pairs, isolated self-interstitials and interstitials in clusters in Mo-Nb system with different Nb concentration of 0%, 25%, 50%, 75% and 100% mole fraction of Nb atoms. It is evident that both the number of Frenkel pairs and isolated self-interstitials increase (Fig. 4(a)) continuously as the Nb content rises, but with less interstitials in clusters (Fig. 4(b)). It is until the Nb content reach to 50%~75% that the ability of clusters formation resistance tends to be saturated (see Fig. 4(b)), but the number of Frenkel

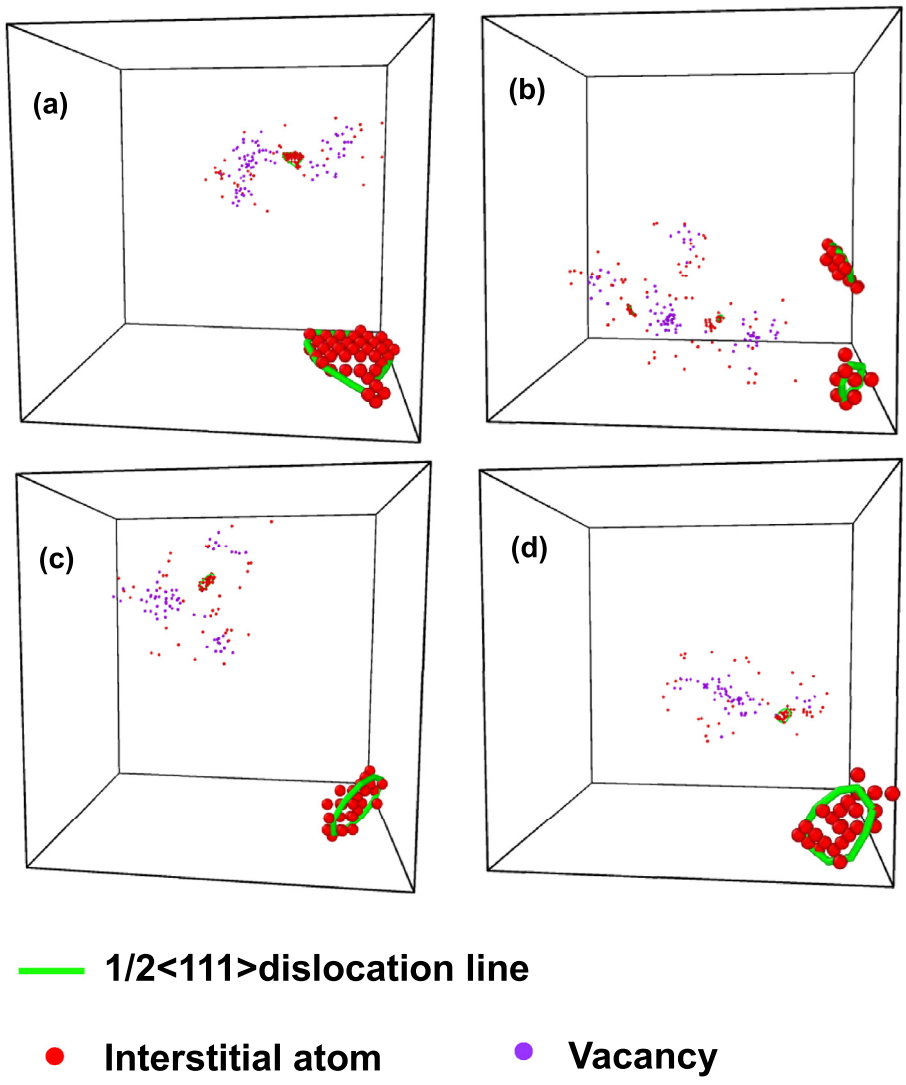

Fig. 2. 3D atomic configure of defects survived in (a) Mo, (b) MoNb, (c) MoNbTa and (d) MoNbTaW when undergone a 50 keV displacement cascade.

pairs still increase. However, if we increase the Nb concentration up to 100% or pure Nb metal, the number of interstitials in clusters with size 2–10 grows sharply, even higher than that of elemental Mo, leading to a sudden reduction of isolated self-interstitals. Obviously, besides the alloy elemental concentrations and types, the compositional heterogeneity should play a significant role in radiation tolerance of bcc CCAs.

To address this issue, we compared the primary radiation damage behaviors of three different equi-atomic MoNb binary CCAs. The three CCAs only differ in the compositional arrangement. They are B2 periodic arrangement structure, random solution structure (RSS) and local chemical ordering structure (LCO). Here, B2-MoNb CCA has "man-made" periodic site lattice site-occupation of Mo and Nb atoms, which is very spatial homogeneous compositional distribution. The LCO-MoNb CCA is obtained from the equilibrium configurations after annealing the RSS-MoNb CCA with the help of Monte Carlo (MC) simulations at 300 K, showing chemical short-range ordering. The RSS-MoNb CCA presents ideal CCA. The corresponding statistics of surviving Frenkel pairs and interstitials in clusters of these three CCAs after the 30 keV displacement cascade is shown in Fig. 5. The number of Frenkel pairs of three type of MoNb is similar, in which RSS-MoNb is slightly less. In addition, the MoNb CCAs with compositional heterogeneity including RSS-MoNb and LCO-MoNb show less interstitial atoms in clusters with size of 2–10. Note that the LCO-MoNb shows the best performance of suppressing interstitial clusters formation among the three CCAs, even no larger clusters (size of 11–30).

4. Discussions

Previous studies on Ni-based fcc HEAs have indicated that the good radiation resistance of CCAs is related to their unique slower energy dissipation and lower defect cluster binding energy compared with elemental materials [11], both of which are based on the ideal CCAs with perfect random solid-solution state. However, even for ideal CCAs, Jin et.al. pointed out that the radiation damage resistance directly correlates with the heterogeneity of defect diffusion due to the randomness nature of lattice site-occupation [46]. Our simulation results also suggest the important role of alloying elements as well as its spatial heterogeneity. In the following, we will focus on the above two factors and how to use them to design new bcc CCAs with better radiation tolerance.

4.1. Alloying elements

We first analyzed the effect of alloying elemental types in the radiation damage resistance. Here, we focus on the three Mo-based

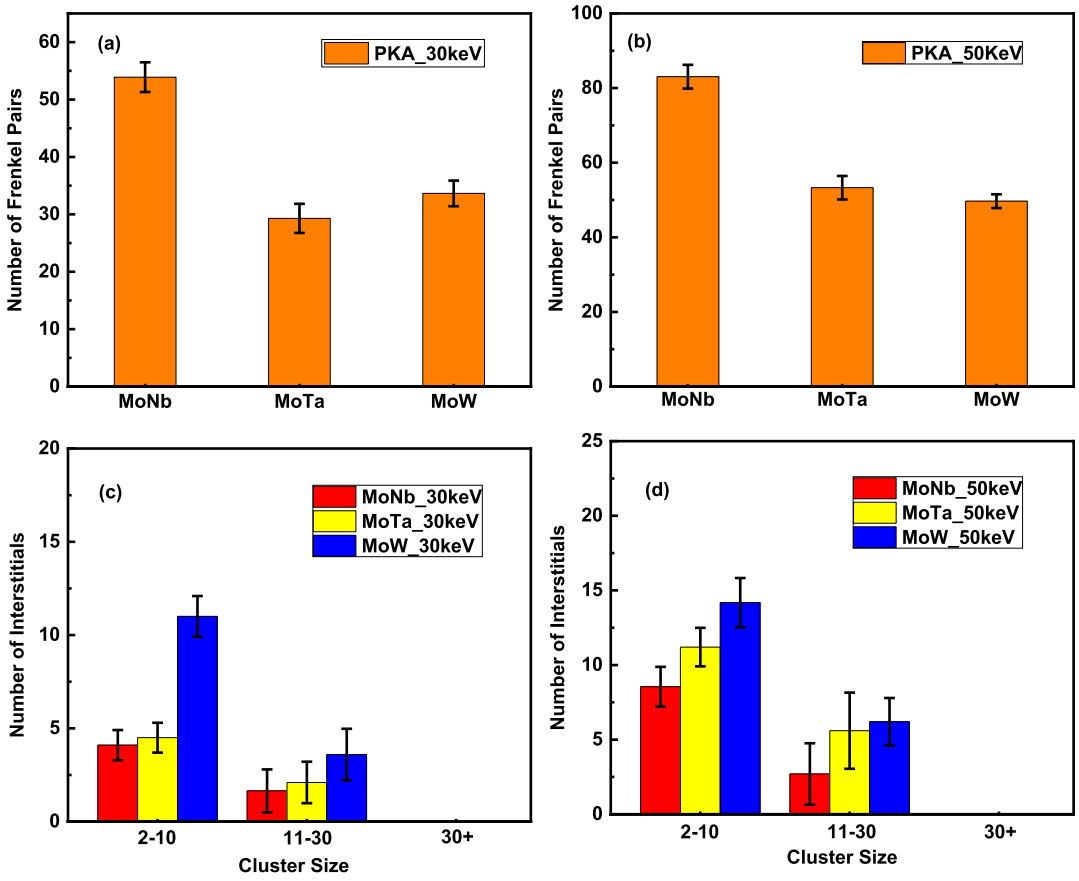

Fig. 3. Comparison of irradiation-induced damage in equi-atomic MoNb, MoTa and MoW CCAs. (a-b) Number of surviving Frenkel pairs at cascade energy of 30 keV and 50 keV. (c-d) Number of interstitials in different sizes clusters at cascade energy of 30 keV and 50 keV.

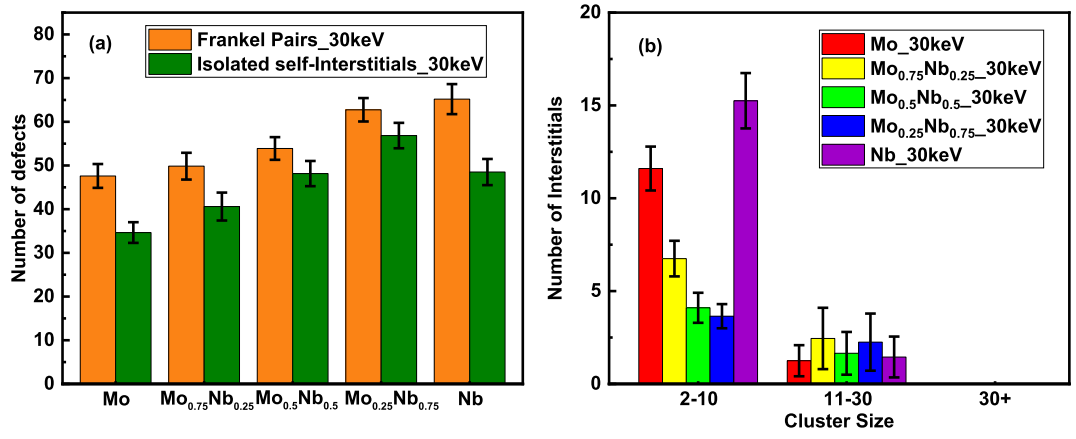

Fig. 4. Comparison of irradiation-induced damage in Mo, $Mo_{0.75}Nb_{0.25}$, $Mo_{0.5}Nb_{0.5}$, $Mo_{0.25}Nb_{0.75}$ and Nb. (a) Number of surviving Frenkel pairs and isolated self-interstitials at cascade energy of 30 keV. (b) Number of interstitials in different sizes clusters at cascade energy of 30 keV.

binary CCAs, which are MoNb, MoTa and MoW. In Fig. 3, we have shown that the three CCAs have quite different radiation damage behaviors. In particular, MoNb CCA shows significant number of interstitial atoms but only a few interstitials in clusters after a displacement cascade. Therefore, we first calculated the self-interstitials formation energy of three binary CCAs. Different from pure elements or dilute alloys, the self-interstitials formation energy in bcc CCAs is quite different from one place to another. In this scenario, bcc CCAs have wide range of local self-interstitials formation energy, i.e., the self-interstitials formation energy is not a constant value. Instead, the value of formation energy can cross several eV.

The probability distribution of self-interstitials formation energy in three binary CCAs is compared in Fig. 6(a), (b) and (c). Among the three CCAs, MoNb has the lowest self-interstitials formation energy, in the region of 3–5.5 eV, and the interval of MoTa and MoW is around 4.9–6.5 eV, 7–9.1 eV, respectively. It is consistent with our finding that MoNb CCA has the most Frenkel pairs but the MoW CCA has the least ones at 50 keV(Fig. 3(b)). Besides, we note that there exist considerable gaps of self-interstitials formation energy between the two principal elements in MoNb and MoW CCAs.

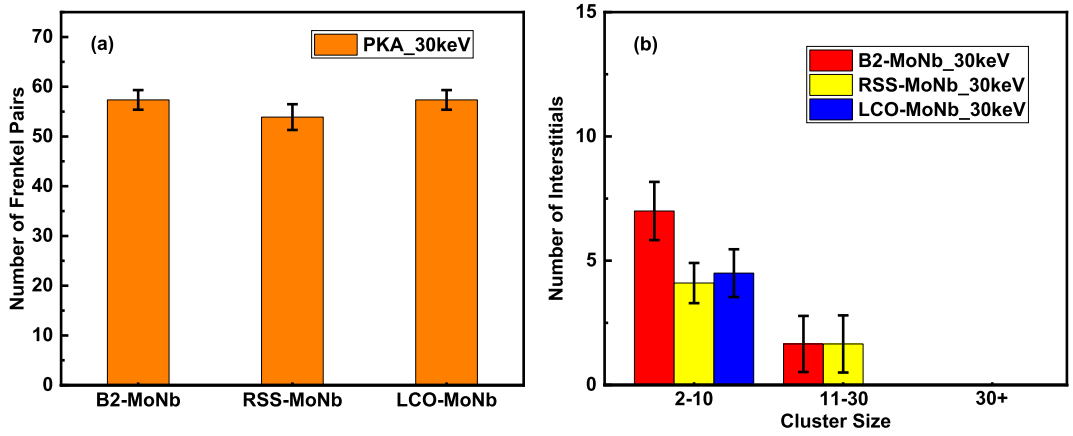

Fig. 5. Comparison of irradiation-induced damage in B2-MoNb, RSS-MoNb and LCO-MoNb at cascade energy of 30 keV. (a) Number of surviving Frenkel pairs at cascade energy of 30 keV. (b) Number of interstitials in different sizes clusters at cascade energy of 30 keV.

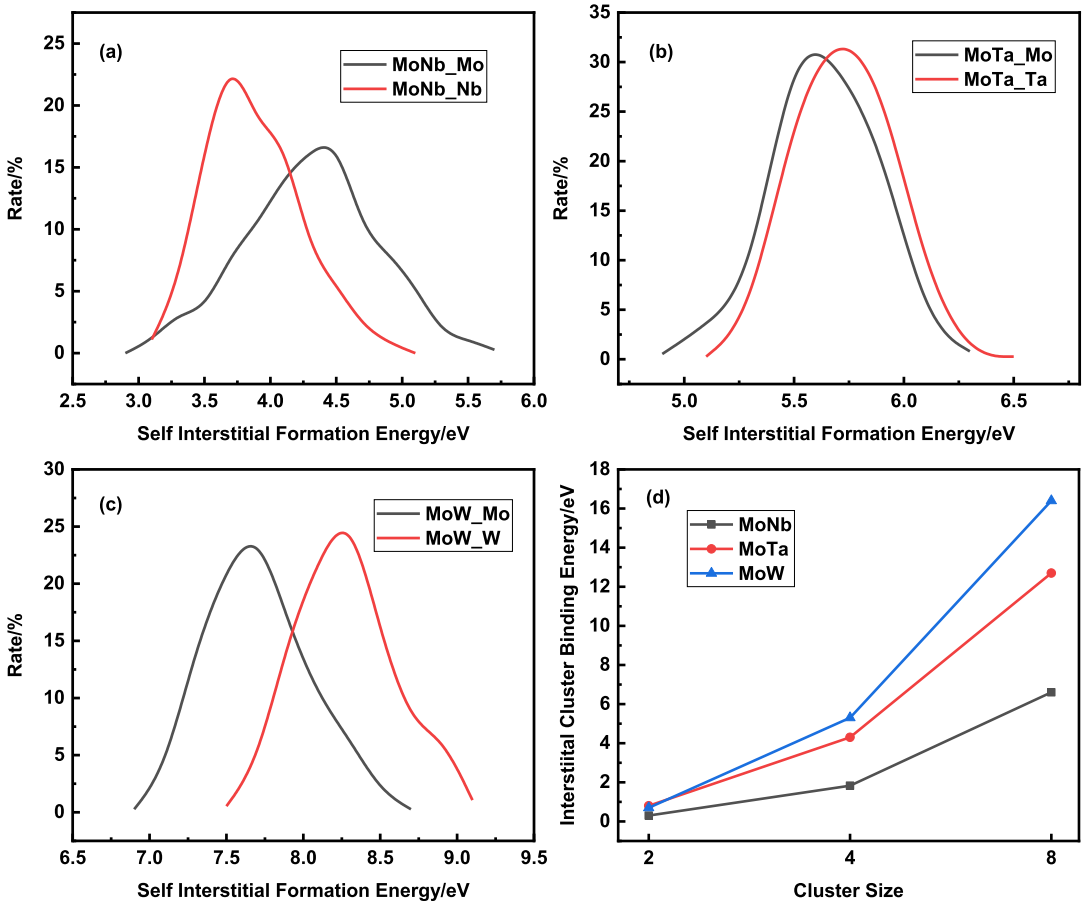

Fig. 6. Probability distribution of self-interstitial formation energy and cluster binding energy in three binary CCAs. (a)-(c) Probability distribution of local self-interstitial formation energy in MoNb, MoTa and MoW CCAs. (d) The average binding energy of interstitial clusters of different sizes in MoNb, MoTa and MoW CCAs.

The formation energy of Nb interstitials is lower than Mo in MoNb system but the opposite in MoW system. With the increase of Nb concentration, more locations in MoNb systems possess low formation energy of self-interstitial, facilitating the formation of Frenkel pairs (Fig. 4(a)). Also, it helps use explain the data of chemical concentrations shown in Table 2 (we will discuss it later).

Besides, we also calculated the binding energy of interstitial clusters with the size of 2, 4 or 8 for the three CCAs in Fig. 6(d). The results are in good agreement with the radiation damage data in Fig. 3(c) and (d) where MoW> MoTa > MoNb sorted by the number of interstitials in clusters. In Fig. 6(d), MoW CCA has the highest binding energy of interstitial clusters while MoNb has the lowest one, and MoTa is in between. Often, the higher the cluster binding energy, the more and larger clusters can survive. It also helps us to understand why MoTa CCA has less number of surviving Frenkel pairs than MoW at 30 keV(Fig. 3(a)), i.e., the interstitial atoms in MoW CCA are more prone to be clustering than MoTa, which retards the interstitial-vacancy annihilation, giving rise to more surviving Frenkel pairs. These suggest that both the formation energy of self-interstitials and binding energy of interstitial

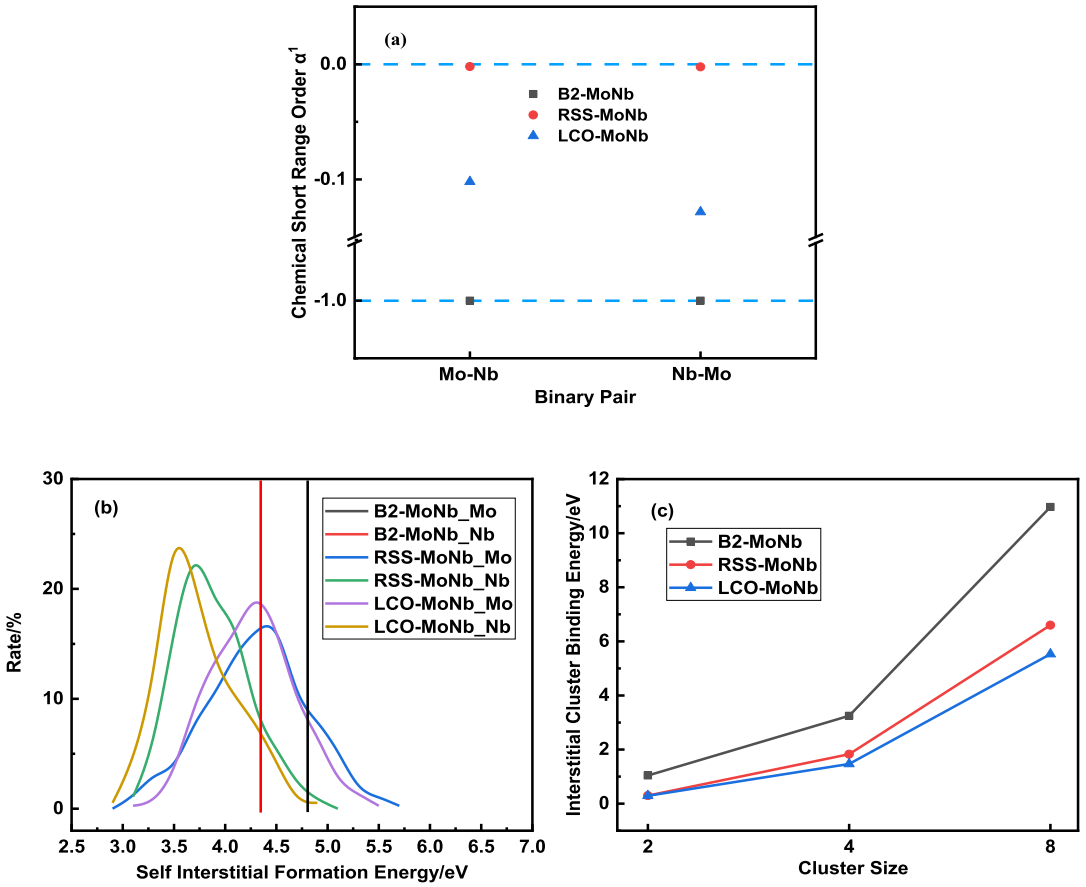

Fig. 7. Comparison of pairwise chemical short-range order parameter, formation energy of self-interstitials and binding energy of interstitial clusters in B2-MoNb, RSS-MoNb and LCO-MoNb. (a) Pairwise chemical short-range order parameter for the first nearest-neighbor shell of the central atom. (b) Probability distribution of self-interstitials formation energy. (c) Binding energy of interstitial clusters. (B2 means B2-type periodic arrangement, RSS is random solid solution and LCO represents local chemical ordering).

Table 2
Local chemical concentration of regions around the isolated self-interstitials and interstitial clusters in MoNb, MoTa and MoW CCAs.

	MoNb	MoTa	MoW
Regions around isolated self-interstitials	Mo:30% Nb:70%	Mo:52% Ta:48%	Mo:60% W:40%
Regions around interstitial clusters	Mo:46% Nb:54%	Mo:45% Ta:55%	Mo:56% W:44%

clusters can serve as order parameters to guide the selection of alloying elemental types for a better radiation tolerance.

4.2. Compositional heterogeneity

Before studying the effect of compositional heterogeneity, we first analyzed the correlation between surviving local defects and chemical concentrations. Here, we show the local chemical concentrations around isolated self-interstitials and interstitial clusters of three binary CCAs, which are equi-atomic MoNb, MoTa and MoW, as listed in Table 2. We find quite different features of local chemical concentrations for regions of isolated self-interstitials and interstitial clusters. Among the three different CCAs that undergone the same 30 keV displacement cascade, the local chemical concentrations of regions near isolated self-interstitials in MoNb and MoW are largely departed from the equi-atomic ratio while no obvious segregation observed in MoTa system. In contrast, nano-regions around the interstitial clusters show local chemical concentrations that are not far from the global average concentration. Simutanously, the three binary CCAs show quite different formation behaviors of self-interstitials. Self-interstitials in MoNb CCA prefer to locate or be formed at the Nb-rich regions while MoW CCA shows self-interstitials located at Mo-rich regions. However, MoTa CCA has no obvious preference. All these indicate that local chemical concentration or compositional heterogeneity governs the formation of radiation induced point defects. Then, a question naturally rises about what the latent variables given by the compositional heterogeneity determines the radiation damage.

We then measure the tendency of local segregation for the three types of MoNb CCAs in Fig. 5 by calculating the corresponding Warren-Cowley SRO parameters, α [39]. We only focused on the first nearest neighbor spacing. Here, α ranges from -1 to 0, where 0 means the complete random and disorder, -1 means complete periodic arrangement. Other values between -1 and 0 indicate a certain degree of local segregation. As shown in Fig. 7(a), $\alpha^1_{\mathrm{Mo-Nb}}$ and $\alpha^1_{\mathrm{Nb-Mo}}$ are only slightly negative (-0.002) for RSS-MoNb with almost ideal solid-solution. However, the absolute value of Warren-Cowley SRO parameter is much larger in LCO-MoNb, indicating considerable Mo-Nb ordering or local segregation. Both $\alpha^1_{\mathrm{Mo-Nb}}$ and $\alpha^1_{\mathrm{Nb-Mo}}$ of "man-made" B2-MoNb are -1, a complete periodic arrangement.

Subsequently, we analyzed how the self-interstitials formation energy and cluster binding energy correlated to the local chemical environments. In Fig. 7(b), we show the probability distribution of self-interstitial formation energy of three types of MoNb CCAs. The self-interstitial formation energy of B2-MoNb has constant values. Instead, the compositional heterogeneity renders both RSS-MoNb

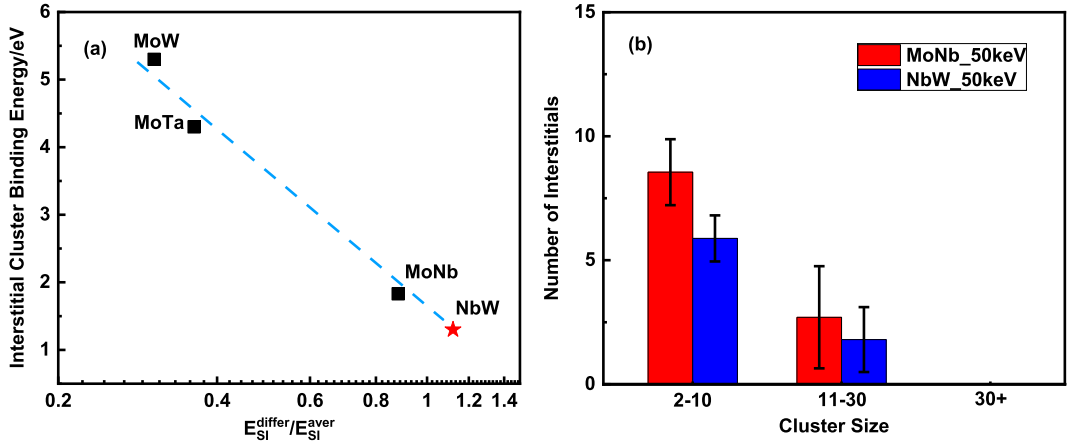

Fig. 8. Prediction of clusters binding energy in binary CCAs and comparison of radiation induced interstitial clusters between MoNb and NbW. (a) The relationship between $E_{SI}^{differ}/E_{SI}^{aver}$ and interstitial cluster binding energy in binary CCAs. (b) Number of interstitials in different sizes clusters at cascade energy of 50 keV.

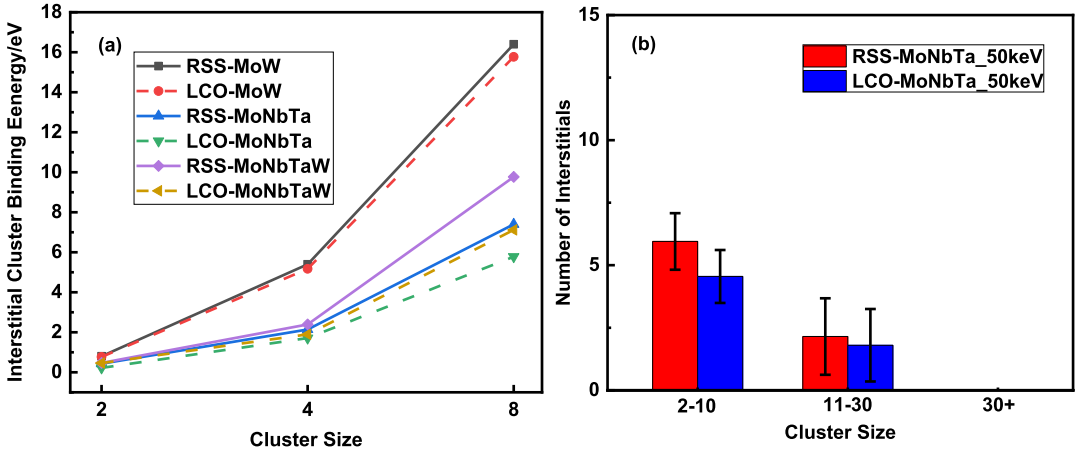

Fig. 9. Comparison of interstitial cluster binding energy and cluster resistance between CCAs in RSS and LCO state. (a) Interstitial cluster binding energy of MoW, MoNbTa and MoNbTaW in RSS and LCO state. (b) Number of interstitials in different sizes clusters between RSS-MoNbTa and LCO-MoNbTa at cascade energy of 50 keV.

and LCO-MoNb a wider range of local defect formation energies, the interval or variance of which is related to the intensity of their local fluctuations. It is found that a larger proportion of locations have lower formation energy than B2-MoNb, which help to trap the moving self-interstitials and may retard the formation of self-interstitial clusters. Fig. 7(c) compared the binding energy of interstitial clusters as a function of cluster size, and B2-MoNb has the highest cluster binding energy which should make interstitial clusters more likely to appear. However, the compositional heterogeneity in MoNb CCAs sharply reduces the clusters binding energy, rationalizing the less interstitials in clusters after the displacement cascade. It is important to note that with the help of local short-range order, the LCO-MoNb shows the lowest binding energy of interstitial clusters, also the best radiation damage resistance.

4.3. Optimization strategy

In order to investigate the degree to which our findings help design bcc CCAs with better radiation tolerance, we performed additional sets of MD calculations of new multi-principal alloys. In this subsection, both the alloying elements and compositional heterogeneity will be tuned to predict new alloys of good radiation tolerance. Then, MD simulations of primary radiation damage will be carried out to validate our predictions.

Firstly, we focus on the screening of new alloying elemental types that can reduce the interstitial clusters binding energy. In Fig. 6, we have shown that equi-atomic MoNb, MoTa and MoW CCAs have quite different cluster binding energies. Here, we propose an empirical formula to build the relationship between the interstitial clusters binding energy and the self-interstitials formation energy of pure elements in equi-atomic binary systems. In this formula, the binding energy of interstitial clusters is described as

$$E_{cluster} \propto \left(\frac{E_{SI}^{differ}}{E_{SI}^{aver}} \right)^{\gamma} \quad (1)$$

where $E_{cluster}$ is interstitial clusters binding energy, E_{SI}^{differ} is the difference between the self-interstitial formation energy of two pure elements and E_{SI}^{aver} is the average self-interstitial formation energy of two pure elements, they are always positive. γ always be negative, means $E_{cluster}$ is inversely proportional to the value in brackets. We fitted the data of Fig. 6(d) in clusters size of 4. As shown in Fig. 8(a), the x-axis increases logarithmically, all the data points located in the same line, indicating a reasonable model. With help of this empirical formula, we can screen new equi-atomic binary bcc CCAs easily using only the self-interstitial formation energy of pure elements. Among the elements Mo, Nb, Ta and W, equi-atomic binary NbW (the red start in Fig. 8(a)) possesses the lowest binding energy of interstitial clusters. Therefore, it should have a better radiation tolerance. This prediction agrees well with our following MD simulations. The number of interstitials in clusters in NbW after the 50 keV displacement cascade is

indeed less than that in MoNb (Fig. 8(b)). It is important to note that the defect formation energy and binding energy can also be calculated by DFT calculations, which have a higher accuracy and better predictability for specific alloy systems.

Secondly, we confirm the role of local chemical ordering in improving the radiation tolerance of multi-principal CCAs in general. Fig. 9(a) compared the binding energy of interstitial clusters among different CCAs between RSS and LCO. For equi-atomic binary MoW, ternary MoNbTa, and quaternary MoNbTaW CCAs, the binding energies of interstitial clusters are all reduced after MC annealing or introducing LCO. Since such effect is the strongest in ternary MoNbTa, we calculated the interstitial clusters accumulation after the cascade in Fig. 9(b). Similar to Fig. 5(b), the number of interstitials in clusters is reduced after the MC annealing. This suggests a general strategy of tailoring the radiation tolerance of bcc CCAs by local chemical ordering. Actually, before the present study, tailoring the degree of LCO has been successfully applied in tuning the stacking fault energies and mechanical properties of HEAs [47,48].

5. Conclusions

In summary, we have investigated the primary radiation damage in bcc concentrated solid-solution alloys by means of large-scale molecular dynamics simulations. Our findings can be summarized as following: (1) With proper alloying elements and local chemical ordering, even binary concentrated solid-solution alloys can show excellent radiation tolerance, not to mention bcc medium or high entropy alloys; (2) The formation energy and cluster binding energy of self-interstitials play an important role in the behavior of primary radiation damage; (3) Compositional heterogeneity can serve as tunable order parameters to tailor radiation tolerance of complex concentrated alloys. Due to the nanoscale chemical heterogeneity widely found in different solution concentrated alloys, our findings are expected to apply to high entropy alloys in general.

Credit author statement

Hongjiang Li: Simulation, Writing - original draft.
Long Zhao: Data analysis.
yang Yang: Writing - editing.
Hongxiang Zong: Conceptualization, Writing - review & editing.
Xiangdong Ding: Hardware support, Supervision.

Declaration of Competing Interest

The authors declare that they have no known competing financial interests or personal relationships that could have appeared to influence the work reported in this paper.

Acknowledgments

This work was supported by Key Technologies R&D Program (2017YFB0702401), the National Natural Science Foundation of China (51320105014, 51871177 and 51931004) and the 111 project 2.0 (BP2018008).

Supplementary materials

Supplementary material associated with this article can be found, in the online version, at doi:10.1016/j.jnucmat.2021.153140.

References

[1] J.W. Yeh, S.K. Chen, S.J. Lin, J.Y. Gan, T.S. Chin, T.T. Shun, C.H. Tsau, S.Y. Chang, Nanostructured high-entropy alloys with multiple principal elements: novel alloy design concepts and outcomes, Adv. Eng. Mater. 6 (2004) 299–303.
[2] C.J. Tong, M.R. Chen, J.W. Yeh, et al., Mechanical performance of the Al x CoCrCuFeNi high-entropy alloy system with multiprincipal elements, Metall. Mater. Trans. A. 36 (2005) 1263–1271.
[3] P. Li, Y. Jia, J. Yi, et al., Composition design, microstructure and mechanical properties of novel multiphase Ti–Cu–Ni–Nb complex concentrated alloys, J. Alloy. Compd. 844 (2020) 156175.
[4] O.N. Senkov, S. Rao, K.J. Chaput, et al., Compositional effect on microstructure and properties of NbTiZr-based complex concentrated alloys, Acta. Mater. 151 (2018) 201–215.
[5] O. El-Atwani, N. Li, M. Li, et al., Outstanding radiation resistance of tungsten-based high entropy alloys, Sci. Adv. 5 (2019) eaav2002.
[6] G. Pu, L. Lin, R. Ang, et al., Outstanding radiation tolerance and mechanical behavior in ultra-fine nanocrystalline Al1.5CoCrFeNi high entropy alloy films under He ion irradiation, Appl. Surf. Sci. 516 (2020) 146129.
[7] D. Patel, M.D. Richardson, B. Jim, et al., Radiation damage tolerance of a novel metastable refractory high entropy alloy V2.5Cr1.2WMoCo0.04, J. Nucl. Mater. 531 (2020) 152005.
[8] C. Lu, T. Yang, K. Jin, et al., Radiation-induced segregation on defect clusters in single-phase concentrated solid-solution alloys, Acta Mater 127 (2017) 98–107.
[9] C. Lu, L. Niu, N. Chen, et al., Enhancing radiation tolerance by controlling defect mobility and migration pathways in multicomponent single-phase alloys, Nat. Commun. 7 (2016) 13564.
[10] Y. Zhang, G.M. Stocks, K. Jin, et al., Influence of chemical disorder on energy dissipation and defect evolution in concentrated solid solution alloys, Nat. Commun. 6 (2015) 8736.
[11] Y. Lin, T. Yang, L. Lang, et al., Enhanced radiation tolerance of the Ni-Co-Cr-Fe high-entropy alloy as revealed from primary damage, Acta. Mater. 196 (2020) 133–143.
[12] H.S. Do, B.J. Lee, Origin of radiation resistance in multi-principal element alloys, Sci. Rep. 8 (2018) 16015.
[13] F. Granberg, K. Nordlund, M.W. Ullah, et al., Mechanism of radiation damage reduction in equiatomic multicomponent single phase alloys, Phys. Rev. Lett. 116 (2016) 135504.
[14] E. Levo, F. Granberg, C. Fridlund, et al., Radiation damage buildup and dislocation evolution in Ni and equiatomic multicomponent Ni-based alloys, J. Nucl. Mater. 490 (2017) 323–332.
[15] T.N. Yang, C. Lu, G. Velisa, et al., Effect of alloying elements on defect evolution in Ni-20X binary alloys, Acta. Mater. 151 (2018) 159–168.
[16] D.S. Aidhy, C. Lu, K. Jin, et al., Point defect evolution in Ni, NiFe and NiCr alloys from atomistic simulations and irradiation experiments, Acta. Mater. 99 (2015) 69–76.
[17] C. Shan, L. Lang, T. Yang, et al., Molecular dynamics simulations of radiation damage generation and dislocation loop evolution in Ni and binary Ni-based alloys, Comput. Mater. Sci. 177 (2020) 109555.
[18] J. Ke, G. Wei, C. Lu, et al., Effects of Fe concentration on the ion-irradiation induced defect evolution and hardening in Ni-Fe solid solution alloys, Acta. Mater. 121 (2016) 365–373.
[19] K. Jin, H. Bei, Y. Zhang, Ion irradiation induced defect evolution in Ni and Ni-based FCC equiatomic binary alloys, J. Nucl. Mater. 471 (2016) 193–199.
[20] P. Xiu, Y.N. Osetsky, L. Jiang, et al., Dislocation loop evolution and radiation hardening in nickel-based concentrated solid solution alloys, J. Nucl. Mater. 538 (2020) 152247.
[21] D. Sobieraj, J.S. Wróbel, T. Rygier, et al., Chemical short-range order in derivative Cr–Ta–Ti–V–W high entropy alloys from the first-principles thermodynamic study, Phys. Chem. Chem. Phys. 22 (2020) 23929–23951.
[22] R. Zhang, S. Zhao, J. Ding, et al., Short-range order and its impact on the CrCoNi medium-entropy alloy, Nat 581 (2020) 283–287.
[23] Y. Kitsunai, H. Kurishita, T. Kuwabara, et al., Radiation embrittlement behavior of fine-grained molybdenum alloy with 0.2 wt%TiC addition, J. Nucl. Mater. 346 (2005) 233–243.
[24] T.S. Byun, M. Li, B.V. Cockeram, et al., Deformation and fracture properties in neutron irradiated pure Mo and Mo alloys, J. Nucl. Mater. 376 (2008) 240–246.
[25] X.W. Zhou, H.N.G. Wadley, R.A. Johnson, et al., Atomic scale structure of sputtered metal multilayers, Acta. Mater. 49 (2001) 4005–4015.
[26] D.Y. Lin, S.S. Wang, D.L. Peng, et al., An n-body potential for a Zr-Nb system based on the embedded-atom method, J. Phys. Condens. Matter. 25 (2013) 105404.
[27] Z.H. Aitken, V. Sorkin, Y.W. Zhang, Atomistic modeling of nanoscale plasticity in high-entropy alloys, Mater. Res. 34 (2019) 1509–1532.
[28] F. Maresca, W.A. Curtin, Mechanistic origin of high strength in refractory BCC high entropy alloys up to 1900K, Acta Mater 182 (2020) 235–249.
[29] B. Chen, S. Li, H. Zong, et al., Unusual activated processes controlling dislocation motion in body-centered-cubic high-entropy alloys, P. Natl. A. Sci. 117 (2020) 16199–16206.
[30] J.F. Ziegler, J.P. Biersack, The stopping and range of ions in matter, in: Treatise on Heavy-Ion Science, Spr., 1985, pp. 93–129.
[31] S.J. Marrink, de. Vries, H. Alex, A.E. Mark, Coarse grained model for semiquantitative lipid simulations, J. Phys. Chem. B. 108 (2004) 750–760.
[32] F. Gao, D. Chen, W. Hu, et al., Energy dissipation and defect generation in nanocrystalline silicon carbide, Phys. Rev. B. 81 (2010) 184101.
[33] S. Plimpton, Fast parallel algorithms for short-range molecular dynamics, Comput. Phys. 117 (1995) 1–19.
[34] A. Stukowski, Visualization and analysis of atomistic simulation data with OVITO–the open visualization tool, Model. Simul. Mater. Sc. 18 (2010) 015012.
[35] K. Nordlund, M. Ghaly, R.S. Averback, et al., Defect production in collision cas-

cades in elemental semiconductors and fcc metals, Phys. Rev. B. Condens. Matter. 57 (1998) 7556–7570.
[36] M.W. Ullah, D.S. Aidhy, Y. Zhang, et al., Damage accumulation in ion-irradiated Ni-based concentrated solid-solution alloys, Acta. Mater. 109 (2016) 17–22.
[37] A. Stukowski, V.V. Bulatov, A. Arsenlis, Automated identification and indexing of dislocations in crystal interfaces, Modelling. Simul. mater. sci. eng. 20 (2012) 085007.
[38] B. Sadigh, P. Erhart, A. Stukowski, et al., Scalable parallel Monte Carlo algorithm for atomistic simulations of precipitation in alloys, Phys. Rev. B. 85 (2012) 184203.
[39] P. Singh, A.V. Smirnov, D.D. Johnson, Atomic short-range order and incipient long-range order in high-entropy alloys, Phys. Rev. B. 91 (2015) 224204.
[40] D. Chen, F. Gao, W.Y. Hu, et al., Migration of Cr-vacancy clusters and interstitial Cr in α-Feusing the dimer method, Phys. Rev. B. 81 (2010) 064101.
[41] T.D. de la Rubia, R.S. Averback, R. Benedek, et al., Role of thermal spikes in energetic displacement cascades, Phys. Rev. Lett. 59 (1987) 1930–1933.
[42] A.F. Calder, D.J. Bacon, A.V. Barashev, et al., On the origin of large interstitial clusters in displacement cascades, Philos. Mag. 90 (2010) 863–884.
[43] F.A. Garner, M.B. Toloczko, B.H. Sencer, Comparison of swelling and irradiation creep behavior of fcc-austenitic and bcc-ferritic/martensitic alloys at high neutron exposure, J. Nucl. Mater. 276 (2000) 123–142.
[44] B.H. Sencer, G.S. Was, M. Sagisaka, et al., Proton irradiation emulation of PWR neutron damage microstructures in solution annealed 304 and cold-worked 316 stainless steels, J. Nucl. Mater. 323 (2003) 18–28.
[45] J. Fu, Y. Chen, J. Fang, N. Gao, et al., Molecular dynamics simulations of high-energy radiation damage in W and W–*Re* alloys, J. Nucl. Mater. 524 (2019) 9–20.
[46] M. Jin, P. Cao, M.P. Short, Thermodynamic mixing energy and heterogeneous diffusion uncover the mechanisms of radiation damage reduction in single-phase Ni-Fe alloys, Acta. Mater. 147 (2018) 16–23.
[47] J. Ding, Q. Yu, M. Asta, et al., Tunable stacking fault energies by tailoring local chemical order in CrCoNi medium-entropy alloys, P. Natl. A. Sci. 115 (2018) 8919–8924.
[48] Q.J. Li, H. Sheng, E. Ma, Strengthening in multi-principal element alloys with local-chemical-order roughened dislocation pathways, Nat. Commun. 10 (2019) 3563.